Energy and Power Engineering, 2022, 14, 13-34
https://www.scirp.org/journal/epe
ISSN Online: 1947-3818
ISSN Print: 1949-243X

Optimization of Losses Joule in the Congolese Electrical Network Integrated with the Energy Pool of Central Africa in the PEAC Acronym

Mathurin Gogom*, Courad Onesime Tsahat Oboulhas, Nianga Apila, Anedi Oko Ganongo, Désiré Lilonga-Boyenga

Laboratoire de Génie Electrique et Electronique, Ecole Nationale Supérieure Polytechnique, Université Marien Ngouabi, Brazzaville, Congo

Email: *mathuringogom@gmail.com

How to cite this paper: Gogom, M., Tsahat Oboulhas, C.O., Nianga Apila, Oko Ganongo, A. and Lilonga-Boyenga, D. (2022) Optimization of Losses Joule in the Congolese Electrical Network Integrated with the Energy Pool of Central Africa in the PEAC Acronym. *Energy and Power Engineering*, **14**, 13-34.
https://doi.org/10.4236/epe.2022.141002

Received: November 8, 2021
Accepted: January 21, 2022
Published: January 24, 2022

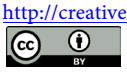

Abstract

Joule losses in the power grids are a factor in the degradation of power grid equipment (lines and transformers), but also a shortfall for power companies, which must maximize their revenues. This is why in this article we present a study on the optimization of joule losses in a meshed electricity network interconnected to a very high voltage power line crossing Congolese territory for nearly one thousand five hundred (1500) kilometers. The value of interconnections no longer needs to be demonstrated in view of these technical, economic and social advantages. The object of this study is to assess the optimal node where the interconnection can be achieved which would cause fewer joule losses in the networks to be interconnected on this line. Indeed, it can have several possible nodes where the interconnection can be carried out, so it is necessary to simulate each configuration in order to evaluate the losses using the hybrid method including the genetic algorithm to provide different configurations and the Newton Raphson algorithm. Advanced integrating FACTS devices in this case STATCOM to perform load flow. The results are interesting because by injecting electrical energy to the network or to the line to the same selected, the joule losses are within the standards provided by the International Electrotechnical Commission.

Keywords

Interconnection, Joule Losses, Configuration, Genetic Algorithm, Newton Raphson Algorithm, FACTS and Load Flow

1. Introduction

Joule losses in electrical networks are not only a degradation factor, but also a

shortfall for electricity companies. The standards require that these losses cannot exceed 3% of the power consumed in the electrical transmission networks and 5% in the electrical distribution networks [1].

As part of the Central Africa Energy Pool PEAC acronym, several national electrical networks will be connected in order to extract or inject electrical energy. In view of the geographical position of certain countries, the transmission and interconnection line will cross a good part of their territory like the Congo. Consequently, the interconnection can generate as many Joule losses thus causing technical and economic inconvenience to the companies in charge if the location is poorly chosen. Thus, it is essential to choose an optimal location where the interconnection can be made to cause fewer joule losses.

Indeed, when the physical flows of electrical energy pass over long distances, the joule losses resulting from this transit are significant, because of the high resistances due to the length of the conductors and the current intensities which pass through them. To optimize these losses due to this transit, the choice of location to achieve the interconnection is essential.

In view of the problem of interconnection in this context, the joule losses should be optimized through an optimal choice of the interconnection node. To do this, we will use a hybrid algorithm: genetic algorithms and the advanced Newton Raphson algorithm using FACTS (Flexible Alterning Current Transfer Systems) [2] [3] [4] [5] and [6]. The genetic algorithms realize the possible configurations while the advanced Newton Raphson algorithm using FACTS performs the load flow calculation, of which the objective is to select an optimal configuration [2] [3] [4] [5] and [6]. This hybrid algorithm is transcribed in the Matlab environment and an application is made on the interconnection of the Congolese network to the PEAC.

The expected results of this study are the selection of an optimal configuration and the evaluation of the joule losses which would obey the standards provided by the International Electrotechnical Commission.

2. Theoretical Study on Joule Losses

When a line or transformer is traversed by electric current, there are losses of power and electrical energy which must be within the limits prescribed by the standards. In this paragraph, we will talk about the main losses.

2.1. Line Losses

The transport of electric current through a power line is subject to loss of power and energy. These losses are due to:

- The resistivity of the conductors causing the joule losses;
- The crown effect.

2.1.1. Joule Losses

They constitute the main component of transport losses. These losses are caused by the current flowing in the lines. Consider **Figure 1** below; the power lost by

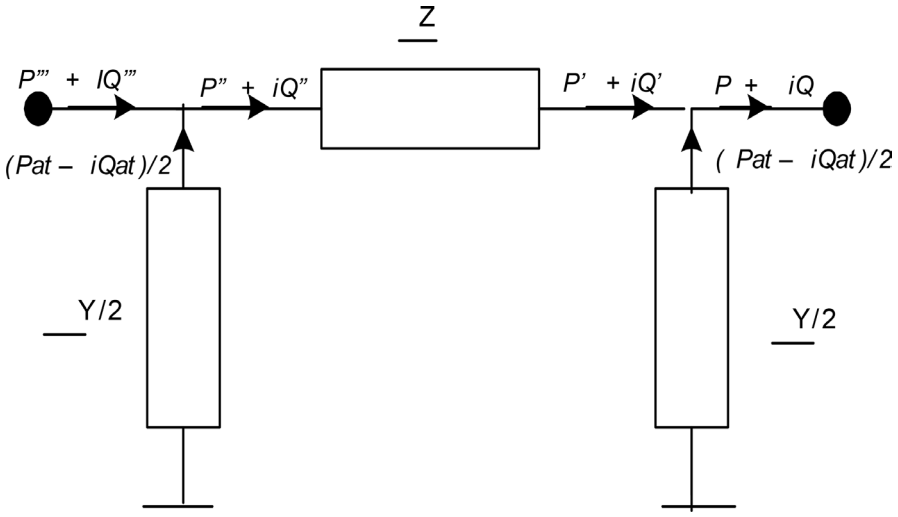

Figure 1. Model of a line describing the losses.

the Joule effect can be calculated in two ways [7] and [8]:

At the start of the line:

$$\Delta P_l = 3R_l I^2 = 3R_l \left(I_a^2 + I_r^2\right)$$

$$P'' = \sqrt{3}U_1 I\cos\varphi_1 = \sqrt{3}U_1 I_a \quad \text{that is} \quad I_a = \frac{P_c''}{\sqrt{3}U_1}$$

$$Q'' = \sqrt{3}U_1 I\cos\varphi_1 = \sqrt{3}U_1 I_r \quad \text{that is} \quad I_r = \frac{Q_c''}{\sqrt{3}U_1}$$

So,

$$\Delta P_l = R_l \frac{P_c''^2}{U_1^2} + R_l \frac{Q_c''^2}{U_1^2} = R_l \frac{S_c''^2}{U_1^2} \tag{1}$$

At the end of the line:

$$\Delta P_l = 3R_l I^2 = 3R_l \left(I_a^2 + I_r^2\right)$$

$$P_c' = \sqrt{3}U_2 I\cos\varphi_2 = \sqrt{3}U_1 I_a \quad \text{that is} \quad I_a = \frac{P_c'}{\sqrt{3}U_2}$$

$$Q_c' = \sqrt{3}U_2 I\cos\varphi_2 = \sqrt{3}U_1 I_r \quad \text{that is} \quad I_r = \frac{Q_c'}{\sqrt{3}U_2}$$

So,

$$\Delta P_l = R_l \frac{P_c'^2}{U_2^2} + R_l \frac{Q_c'^2}{U_2^2} = R_l \frac{S_c'^2}{U_2^2} \tag{2}$$

2.1.2. Crown Losses

When a wire is brought to a high electric potential, the field around it can become strong enough to cause ionization of molecules in the air. The ions thus formed are then entrained by the electrostatic force and tend to move along the field lines, which induces leaks. These losses are amplified in wet weather or by precipitation (snow, rain, etc.). The losses by corona effect depend on the ten-

sion of the lines and the amount of precipitation. The study of corona losses is approached by taking into account the characteristics of transmission lines (circuit length and route by voltage level), the frequency of precipitation and experimental data. The losses due to the crown effect are given by the following formula:

$$\Delta P_c = 3GV^2 \tag{3}$$

2.2. Losses in the Transformer

2.2.1. Power Lost by Joule Effect

They constitute the main component of transport losses. These losses are caused by the current flowing through the transformers. For a transformer operating in normal mode in **Figure 2**, the active power lost in it is determined as follows [7] and [8]:

$$\Delta P_T = 3R_1 I_1^2 \quad \text{or} \quad \Delta P_T = R_2 I_2^2$$

when the parameters are respectively reduced to primary or secondary. Consider the case where the parameters are reduced to primary,

$$\Delta P_T = 3R_1 I_1^2 \quad \text{avec} \quad \overline{I}_1 = I_{1a} - jI_{1r},$$

$$\Delta P_T = 3R_1 \left(I_{1a}^2 + I_{1r}^2 \right)$$

If we don't know I_{1a} et I_{1r}, but rather P_1, Q_1 et U_1, so we can write:

$$P_1 = \sqrt{3} U_1 I_1 \cos\varphi_1 = \sqrt{3} U_1 I_{1a} \quad \text{that is} \quad I_{1a} = \frac{P_1}{\sqrt{3} U_1}$$

$$Q_1 = \sqrt{3} U_1 I_1 \sin\varphi_1 = \sqrt{3} U_1 I_{1r} \quad \text{that is} \quad I_{1r} = \frac{Q_1}{\sqrt{3} U_1}$$

then

$$\Delta P_T = R_1 \frac{P_1^2}{U_1^2} + R_1 \frac{Q_1^2}{U_1^2} = R_1 \frac{S_1^2}{U_1^2} \tag{4}$$

2.2.2. Power Lost in Iron

We call iron losses the sum of the losses by hysteresis and the losses by eddy current. The magnetization of the transformer sheets is the cause of the iron losses. It is given by the formula below:

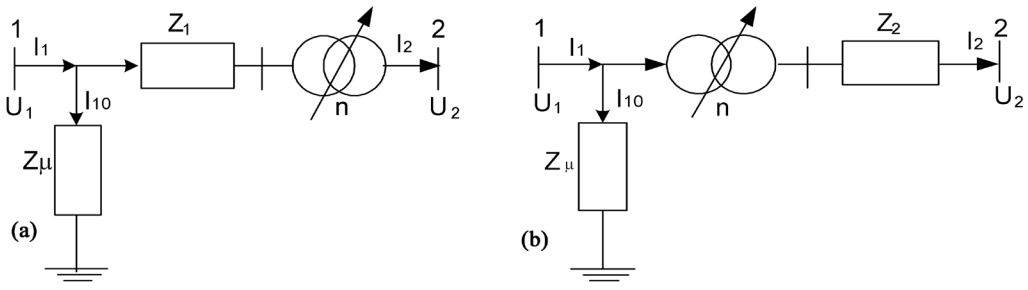

Figure 2. transformer model whose parameters are reduced: (a) to the primary and (b) to the secondary.

$$P_{10} = \frac{V^2}{R_\mu} \tag{5}$$

2.3. Allowable Loss Rate

It is traditional to express losses as a rate. This rate allows comparisons between companies, and within a company comparisons between years. These rates have also allowed some authors to establish permissible rate ranges.

By definition, the optimal rate of technical losses is that which is reached when all the reinforcement works are profitable with regard to the economic parameters adopted (loss costs, reference costs of the works, discount rate, valuation of the quality of supply, …) were completed on time.

The acceptable levels for energy losses, both for an entire electrical system and for each of these main components are defined by experts as follows [1]:

- For the entire electrical system (generation, transmission and distribution), 9% to 10% is adequate and 17% the maximum tolerable;
- For the transport network, 2% to 3% is suitable and 6% the maximum tolerable.

These rates are all based on the total energy injected into the transmission network.

2.4. Hybrid Optimization Method

The hybrid optimization method combines genetic algorithms and Newton Raphson's advanced method including FACTS.

2.4.1. Genetic Algorithm

This method is selected because of its speed of convergence and precision of the results compared to other metaheuristic methods [2] and [3]. In this subsection, we describe the different stages of genetic algorithms within the framework of our study.

1) Initial population and coding

The initial population which constitutes the set of network configurations is generated in a random manner. Its size results from a compromise between the calculation time, the number of variables to be optimized and the quality of the populations found. It is advisable to increase the size in order to promote the intensification and diversification of individuals or configurations.

The coding of the configurations is an important parameter of the method. The configurations are represented in the form of strings containing characters or (genes) of a determined alphabet. The encoding must be tailored to the problem in order to limit the size of the search space by producing valid solutions as often as possible when applying search operators. The representation must be such that the search operators are efficient in reproducing the sought solutions with a good probability.

In this work, we use binary encoding in which each solution is represented by a string of 0 or 1 called bit. The genetic algorithm often uses this representation

when dealing with complex structures. The number of bits is equal to the number of nodes where the interconnection can be made. The string takes the character or (alphabet) 0 when the interconnection is not carried out at this node of the electrical network and 1 when it is carried out. Each character corresponds to a number of the desired node.

2) Evaluation

The evaluation is the most time-consuming part of the algorithm, because it needs the results of the load balancing calculation. Once the initial population is created, each individual (configuration) is evaluated against the optimization objective considered. For the search for an optimal interconnection node from which the losses are minimal, the evaluation consists of a calculation of the losses in the network by the Newton Raphson method in order to deduce the evaluation function. In our case, the evaluation function, called the fitness function is given by [3] [4] and [5]:

$$f_{it_i} = \frac{1}{p_m + \frac{x_{\text{cali}} - x_{\min}}{x_{\max} - x_{\min}} p_c} \tag{6}$$

where p_m is the probability of mutation, p_c the probability of crossing, x_{cali} the losses calculated for each configuration, $x_{\max}$ the upper limit of joule losses in networks and $x_{\min}$ the lower limit of joule losses in networks.

According to this formulation, the fitness function can take values between 0 and 10 for the best configurations, and greater than 10 for the less good. The population at a given time of the algorithm is called generation. Once the generation has been assessed, individuals are ranked according to the value of their fitness function.

3) Selection

The selection of individuals for the intermediate generation is carried out, in our case, by the draw on the biased roulette in which each individual has a proportional share to his fitness function. This selection technique allows good individuals to be part of the next generation, but it also avoids the premature convergence of the algorithm. It is necessary to maintain sufficient genetic diversity in the population to guarantee the genes that can be subsequently. Indeed, any individual can transmit genes to their descendants which, when combined with others, can be interesting.

4) Crossing

After selection, the crossing of two individuals to give two children can occur with a probability between 0.8 and 1. In this research work, the multipoint crossing is applied. For this, a few points are drawn randomly, and between these points, the nodes of the two solutions (configurations) are exchanged. As mentioned in [2] and [3], two interconnections do not need to be made. An example of a multipoint crossing is shown in **Figure 3**.

5) Mutation

In our case, the mutations can take place on the characters of the two chains

(the place of connection and the powers to be exchanged) representing a solution. The mutation effect results in a change of the value of the selected location. The new value is randomly drawn among the possible values. The mutation in several places of each of the two chains is illustrated in **Figure 4**.

A specific mutation probability is applied to each parameter:

p_{mes} for interconnection locations;

p_{mv} for the set point values of the exchanged powers.

These probabilities vary over generations. They increase to promote diversification when the population tends to be represented by only a few dominant individuals. The mutation probability can be between 0.01 and 0.2. The general functioning of the genetic algorithms is given in **Figure 5** [2] and [5].

2.4.2. Advanced Newton-Raphson Method

Advanced Newton-Raphson method is the load balancing calculation performed by including Statcom controllers. This method consists in solving the system of equations at the nodes of the electrical network, given by [2] [3] [4] [5] and [6]:

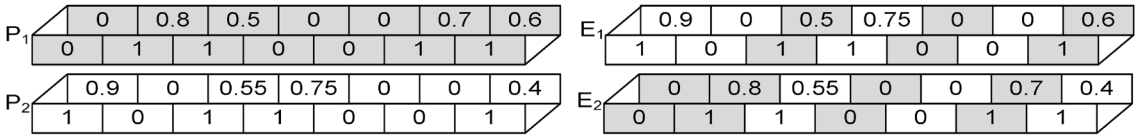

Figure 3. Multipoint crossing of both parents.

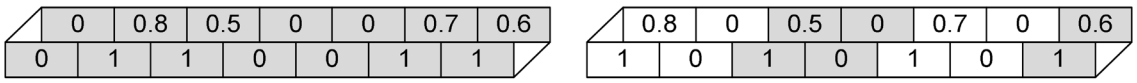

Figure 4. character mutation of two strings.

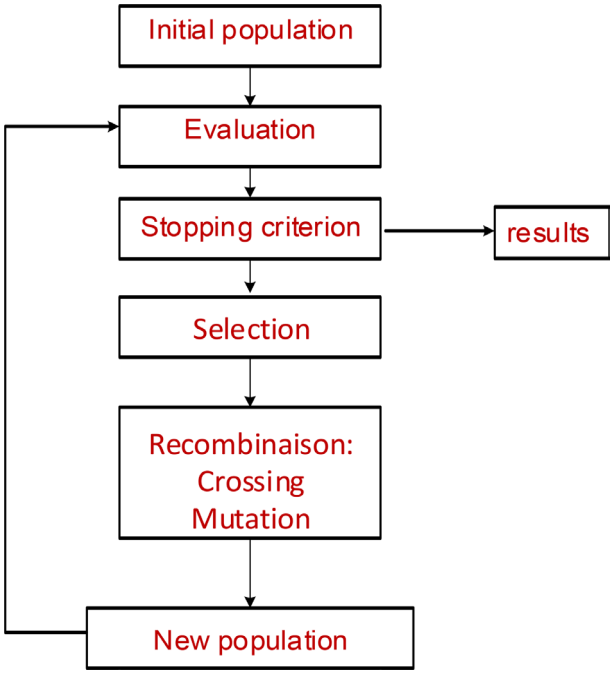

Figure 5. How genetic algorithms work.

$$\begin{cases} P_i = Y_{ii}V_i^2 \cos(\propto_{ii}) + V_i \sum_{k\neq 1}^{n} Y_{ik}V_k \cos(\varphi_i - \varphi_k - \alpha_{ik}) \\ Q_i = Y_{ii}V_i^2 \sin(\propto_{ii}) + V_i \sum_{k=1}^{n} Y_{ik}V_k \sin(\varphi_i - \varphi_k - \alpha_{ik}) \end{cases} \quad (7)$$

This system is linearized and transcribed in the form of a matrix equation to have voltage modules and phases at the nodes of the electrical network. Once these voltage modules and phases have been obtained, the losses in the network are deduced from them using the nodes method. For this, the power transit equations are established in order to deduce the losses [2] [3] [4] [5] and [6]:

$$\begin{aligned} P_{ik} &= G'_{ik}V_i^2 - G_{ik}V_iV_k \cos(\theta_i - \theta_k) + B_{ik}V_iV_k \sin(\theta_i - \theta_k) \\ Q_{ik} &= B'_{ik}V_i^2 - G_{ik}V_iV_k \sin(\theta_i - \theta_k) - B_{ik}V_iV_k \cos(\theta_i - \theta_k) \end{aligned} \quad (8)$$

$$\begin{aligned} P_{ki} &= G'_{ik}V_k^2 - G_{ik}V_iV_k \cos(\theta_k - \theta_i) + B_{ik}V_iV_k \sin(\theta_k - \theta_i) \\ Q_{ki} &= B'_{ik}V_k^2 - G_{ik}V_iV_k \sin(\theta_k - \theta_i) - B_{ik}V_iV_k \cos(\theta_k - \theta_i) \end{aligned} \quad (9)$$

$$\begin{aligned} \Delta P_{ik} &= P_{ik} + P_{ki} = G'_{ik}(V_i^2 + V_k^2) - 2G_{ik}V_iV_k \cos(\theta_i - \theta_k) \\ \Delta Q_{ik} &= Q_{ik} + Q_{ki} = B'_{ik}(V_i^2 + V_k^2) - 2B_{ik}V_iV_k \cos(\theta_i - \theta_k) \end{aligned} \quad (10)$$

where the systems of Equations (3) and (4) are respectively the power transits seen from node *i* and node *k*, and the system of Equation (5) reflects the losses in the network.

2.5. Formulation of the Hybrid Optimization Problem

In this work, we are looking for one of the probable nodes to achieve the interconnection that would cause the minimum Joule losses when the Congolese electrical network is perfectly regulated in voltage [5]. To do this, the objective function is formulated in order to minimize joule losses in the electrical network. The equality constraints are attached (the power equations at the nodes which must obey Kirchhoff's laws) and the inequality constraints are also attached:

- The tensions at the nodes must not deviate sufficiently from the reference values;
- Statcom generators and controllers must be operated close to their operating limits;
- Power transits in the lines must be close to thermal limits.

Thus, the hybrid optimization problem can be formulated by minimizing $f(X,U)$ to deduce the best fitness function f_{it_i} and take into account the following constraints:

$$\begin{cases} g(X,U) = 0 \\ h(X,U) \leq 0 \end{cases} \quad (11)$$

where X is the state vector of the electrical network (modules and voltage phases at the nodes), U the vector representing the variables of the Statcom controllers and the possible auxiliary variables, all considered as state variables and $f(X,U)$

the objective function, representing the joule losses in the electrical network, determined by the method of nodes. Thus, the fitness function given by relation (12) allows to evaluate and select necessary individuals for the recombination.

$$f_{it_i} = \frac{1}{p_m + \dfrac{f(X,U)_{\text{cali}} - f(X,U)_{\min}}{f(X,U)_{\max} - f(X,U)_{\min}} p_c} \tag{12}$$

The relation $g(X,U)$ represents the equality constraints, corresponding to the power injection equations including those of Statcom and $h(X,U)$ the inequality constraints, reflecting the limitations on the equipment in service (generators, lines and Statcom):

- For generators, these limits are expressed by:

$$Q_i^{\min} \le Q_i(V,U) \le Q_i^{\max} \tag{13}$$

Où

$$Q_i^{\min} - Q_i(V,U) \le 0; \tag{14}$$

$$Q_i(V,U) - Q_i^{\max} \le 0;$$

where Q_i is a function of the modules and voltage phases at the i^{th} node and all neighboring nodes. If at the end of the calculation, or during it, the production Q_i exceeds the upper bound $Q_i^{\max}$, we impose:

$$Q_i(V,U) - Q_i^{\max} = 0$$

Similarly, if the production exceeds the lower b $Q_i^{\min}$, we impose:

$$Q_i^{\min} - Q_i(V,U) = 0$$

In both cases, the node of type PV becomes PQ.

- For lines, power flows should not exceed 90% of their respective transfer capability. For each row, the following inequalities are valid

$$S_{ik} \le 0.9 S_{ik}^{\max} + \epsilon_{ik}, \quad 0 \le \epsilon_{ik}$$

$$S_{ik} \le S_{ik}^{\max} + \gamma_{ik}, \quad 0 \le \gamma_{ik} \tag{15}$$

where the quantity S_{ik} is the apparent power across the line ik and ϵ_{ik} and γ_{ik} the non-zero deviation variables if the initial constraints are not respected.

- For nodes, these are V_i voltage, as soft constraints. These voltages V_i are imposed to be around the reference value:

$$V_i^{\min} \le V_i^{\text{ref}} \le V_i^{\max}$$

$V_i^{\min} = 0.95 V_i^{\text{ref}}$ is the minimum acceptable value of the voltage at node i;
$V_i^{\max} = 1.05 V_i^{\text{ref}}$ is the maximum acceptable value of the voltage at node i.

For the static reactive power compensator, the reactive power Q_{STATCOM} can take the values in the range:

$$Q_{C\max} \le Q_{\text{STATCOM}} \le Q_{L\max}$$

The operating principle of the hybrid optimization method is given by the algorithm shown in **Figure 6** [6].

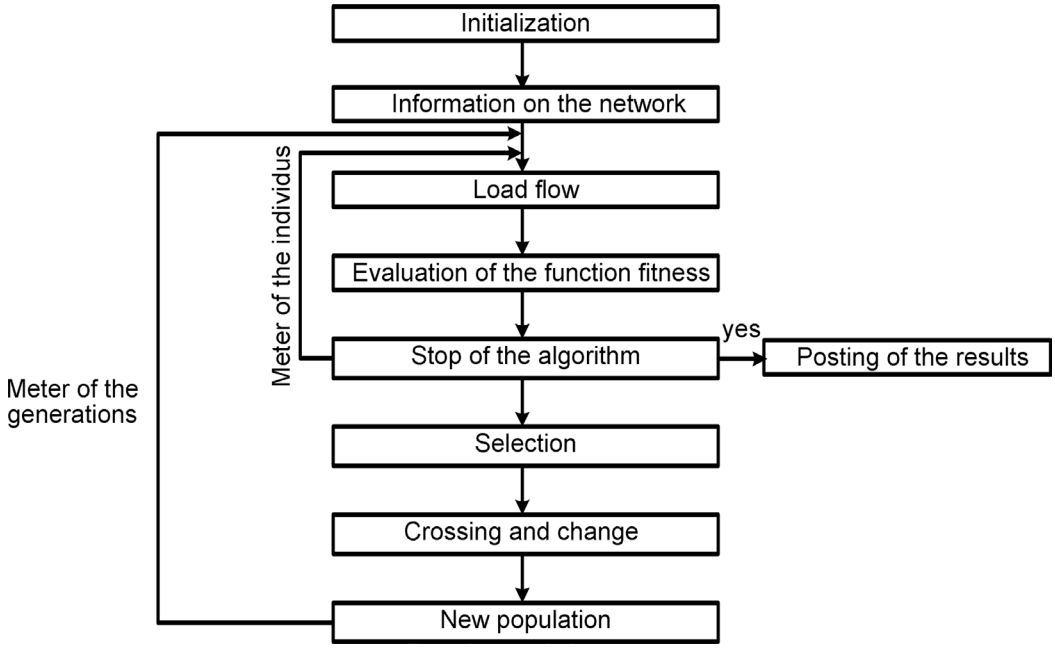

Figure 6. How the hybrid optimization algorithm works.

3. Application to the Congolese Network Integratedin to the PEAC

3.1. Network Characteristics

The integration of the Congolese electricity network into the PEAC will be carried out according to **Figure A1**. For this purpose, four connection points can be envisaged at 400 kV (red line shown in **Figure A2**) [9] [10] and [11]:

- Node 8 in Ouesso (the country's second economic hub) in the north-west of the country is the first point of interconnection of the Congolese network to the PEAC.

This connection has three departures (first departure to supply the locality of Ouesso, second departure to Gabon, Cameroon, Nigeria and other countries and the third departure to RCA and Tchad). At the same time, it could constitute a connection point for the Chollet hydroelectric power station on the border with Cameroon, currently under study with an estimated power of 900 MW;

- Node 3 in Oyo, one of the economic hubs of the Republic of Congo, characterized by high consumption of electrical energy;
- Node 12 in Brazzaville, the political capital of Congo, constitutes the third point of interconnection to the PEAC;
- Node 37 in Pointe Noire, the most important economic hub in the country, represents the fourth interconnection point at PEAC.

This connection point has two purposes: first to guarantee the supply of this industrial zone with electrical energy and secondly to allow the future connection of the Sounda hydroelectric power station with an estimated power of 1200 MW under study. This site is located approximately at 75 km from Pointe-Noire by bird flight. The 400 kV line that crosses the Congo is approximately 1200 km

long in bird flight.

3.2. Modelization

3.2.1. Modeling of the Interconnected Network

Certain electrical networks have particular topologies or configurations, characterized by very varied operating voltages, in particular 400 kV; 220 kV; 110 kV and 30 kV which are the output voltages of the transformers.

Outside the lines whose modeling is simple, that of transformer swath two and three windings is complex. Transformers with two windings will be modeled as lines, while those with three windings will be modeled as two lines supplying two departures [6].

The Z impedances and admittances of the transmission lines are determined such that:

$$\underline{Z} = \underline{z}_0 \cdot l = \left(r_0 + ix_0\right) \cdot l \tag{16}$$

$$\underline{Y} = \underline{y}_0 \cdot l = \left(g_0 + ib_0\right) \cdot l \tag{17}$$

where r_0 and x_0 are the linear resistance and reactance of the transmission line, respectively; g_0 and b_0 the linear conductance and susceptance of the transmission line and l the length of the transmission line.

The Z impedances of the transformers, for their part, are determined such as:

- Transformers with two windings:

$$Z = \frac{U_{ncc}\%U_n}{100\sqrt{3}I_n} \quad \text{that is} \quad \underline{Z} = R + iX \tag{18}$$

$$\text{With} \quad R = Z\cos\varphi_T ; \quad X = Z\sin\varphi_T \quad \text{and} \quad \varphi_T = \tan^{-1}\frac{X}{R}$$

where R and X are the resistance and the leakage reactance of the transformer, respectively; U_{ncc}% the short-circuit voltage as a percentage ; U_n nominal voltage and I_n the nominal current intensity.

- Transformers with three windings:

$$Z_{12} = \frac{U_{12ncc}\%U_{1n}}{100\sqrt{3}I_{1n}}; \quad Z_{13} = \frac{U_{13ncc}\%U_{1n}}{100\sqrt{3}I_{1n}} \quad \text{et} \quad Z_{23} = \frac{U_{23ncc}\%U_{2n}}{100\sqrt{3}I_{2n}} \tag{19}$$

Then, we deduce:

$$R_{12} = Z_{12}\cos\varphi_{12}; \quad R_{13} = Z_{13}\cos\varphi_{13} \quad \text{et} \quad R_{23} = Z_{23}\cos\varphi_{23}$$

$$X_{12} = Z_{12}\sin\varphi_{12}; \quad X_{13} = Z_{13}\sin\varphi_{13} \quad \text{et} \quad X_{23} = Z_{22}\sin\varphi_{23}$$

$$\text{With} \quad \varphi_{12} = \varphi_{13} = \varphi_{23} = \varphi = \tan^{-1}\frac{X_{12}}{R_{12}}$$

The base quantities calculated by the formulas below are summarized in Table below:

$$Z_B = \frac{U_B^2}{S_B} \quad \text{et} \quad Y_B = \frac{1}{Z_B}$$

	S_B (MVA)	U_B (KV)	Z_B (Ω)	Y_B (Ω^{-1})
1	100	400	1600	0.625×10^{-3}
2	100	220	484	2.066×10^{-3}
3	100	110	121	0.826×10^{-3}
4	100	30	9	111.11×10^{-3}

Then, for each quantity, one will calculate its value in pu according to the formula below:

$$\text{pu value} = \frac{\text{Real Value}}{\text{base value}}$$

3.2.2. Statcom Modeling

STATCOM can be modeled by the simplified circuit of the control and compensation system in Figure 7. The modeling of this circuit is based on the following simplifying assumptions [12] [13] [14] and [15]:

- All switches are assumed to be ideal;
- The three voltages of the AC source are balanced;
- All voltage drops in STATCOM are represented by resistor r_p;
- Harmonics caused by the opening and closing action of switches are neglected;
- The leakage inductance of the shunt transformer is represented by the inductance L_p.

The STATCOM device controls:

- The injected voltage V_p in phase with the voltage V_r of the line;
- The voltage phase or the transport angle.

The main purpose of these two operating modes is to control the reactive power passing through the line. The dynamic equations of Statcom are obtained by applying the KIRCHHOFF law relating to the three phases [12] [13] [14] [15]:

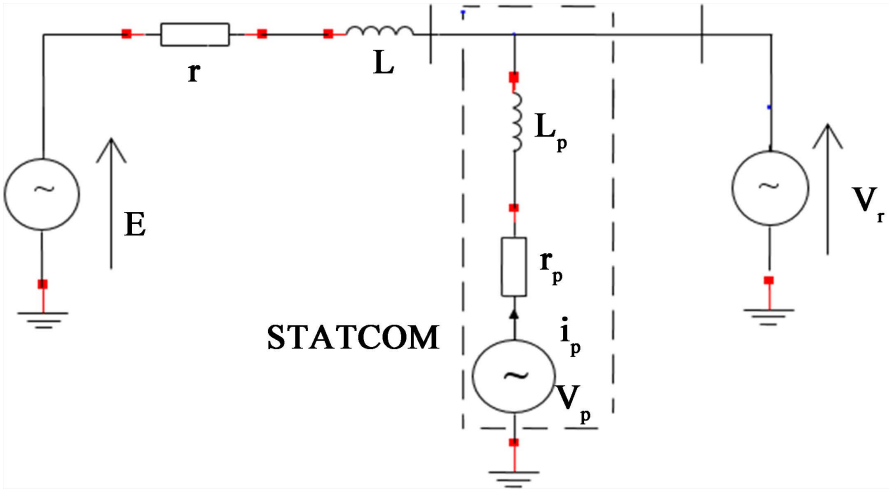

Figure 7. STATCOM model.

$$\begin{cases} \dfrac{\mathrm{d}i_a}{\mathrm{d}t} = -\dfrac{r}{L}i_a + \dfrac{1}{L}\left(V_a - V_{ca} - V_{ra}\right) \\ \dfrac{\mathrm{d}i_b}{\mathrm{d}t} = -\dfrac{r_p}{L_p}i_{pb} + \dfrac{1}{L_p}\left(V_{pb} - V_{cb} - V_{rb}\right) \\ \dfrac{\mathrm{d}i_c}{\mathrm{d}t} = -\dfrac{r_p}{L_p}i_{pc} + \dfrac{1}{L_p}\left(V_{pc} - V_{cc} - V_{rc}\right) \end{cases} \tag{20}$$

where $i_{,abc}$ are the Statcom currents, $V_{,abc}$ are the voltages generated by the inverter, r and L are the resistance and inductance of the Statcom respectively.

The system of Equation (15) can be rewritten in the matrix form (16):

$$\begin{bmatrix} V_{pa} \\ V_{pb} \\ V_{pc} \end{bmatrix} = \begin{bmatrix} r_p + s \cdot L_p & 0 & 0 \\ 0 & r_p + s \cdot L_p & 0 \\ 0 & 0 & r_p + s \cdot L_p \end{bmatrix} \begin{bmatrix} i_{pa} \\ i_{pb} \\ i_{pc} \end{bmatrix} + \begin{bmatrix} V_{ca} + V_{ra} \\ V_{cb} + V_{rb} \\ V_{cc} + V_{rc} \end{bmatrix} \tag{21}$$

Of which i_{pa}, i_{pb} and i_{pc} represent the shunt currents, moreover V_{pa}, V_{pb} and V_{pc} are the voltages generated by the inverter. In matrix form the system (15) becomes:

$$\frac{\mathrm{d}}{\mathrm{d}t}\begin{bmatrix} i_{pa} \\ i_{pb} \\ i_{pc} \end{bmatrix} = \begin{bmatrix} -r_p/L_p & 0 & 0 \\ 0 & -r_p/L_p & 0 \\ 0 & 0 & -r_p/L_p \end{bmatrix} \begin{bmatrix} i_{pa} \\ i_{pb} \\ i_{pc} \end{bmatrix} + \frac{1}{L_p}\begin{bmatrix} V_{ca} + V_{ra} \\ V_{cb} + V_{rb} \\ V_{cc} + V_{rc} \end{bmatrix} \tag{22}$$

3.3. Simulations, Results and Discussion

We simulate the Congolese electricity network interconnected to the PEAC on the basis of Equations (12) to (15). These equations are implemented in the Matlab environment. At the end of this simulation, the program returns the results with the mention "good configuration found" when the objective is reached and the constraints respected on the one hand, and "no solution found" when the objective is not. reached and/or when the constraints are not respected. Ultimately, the ideal interconnection node found is the one from which losses are minimal. The simulation results obtained when the Congolese network absorbs the electrical energy from the PEAC have selected node 12 as the interconnection point and the voltage modules and phases, as well as the injected and absorbed powers are presented in Table A1 and Table A2 in Annex 2. However, the simulation results obtained when the Congolese network injects electrical energy into the PEAC are shown in Table A3 and Table A4 in appendix 2. The results of simulations, when the Congolese network absorbs electrical energy from the PEAC, shown in Table A1 and Table A2 in the appendix show:

- That among the four (4) probable interconnection nodes, node 12 is selected as the interconnection node of the Congolese network to the PEAC, because at this node the joule losses in the Congolese network are equal to 0.22136 pu when it is perfectly compensated.
- That to guarantee the national electricity supply (except rural areas), a quantity of approximately 11.7875 pu including the joule losses in the network is

required, for a national production of 10.56 pu.

So, despite the project to build the hydroelectric dam at Chollet with an installed capacity of 3 pu, the Congo's share, it will still have an energy deficit; therefore it will be able to import 1.25 pu from node 12.

However, the results of simulations, when the Congolese network injects electrical energy into the PEAC, reported in Table A3 and Table A4 in appendix 2 show:

- That among the four (4) probable interconnection nodes, node 12 is always selected as the ideal interconnection node of the Congolese network to the PEAC, because at this node the joule losses in the Congolese network are equal to 1.35814871 pu when it is perfectly compensated;
- That to guarantee the national electricity supply and ensure the injection of electric energy to the PEAC, a national production of 22.56 pu is needed which can be obtained thanks to the construction of the hydroelectric dam of Sounda with a capacity of installed of 12 pu, and therefore the Congo will be able to export 10.7725 pu.

4. Conclusions

The selection of the interconnection node of the Congolese electricity grid at the PEAC was the subject of our study. It was a question of examining the four (4) possible configurations by performing a load distribution calculation integrating STATCOM.

Thus, node 12 was selected in both cases:

- When the Congolese electricity network receives power of 1.25 pu from the PEAC, the joule losses are equal to 0.22136 pu, *i.e.* a rate of 1.62% < 3%, unlike nodes 3, 8 and 37 which respectively cause of losses of 5.75%, 6.3% and 4.81%;
- When the Congolese electricity network injects a power of 10.7725 pu to the PEAC, the joule losses are equal to 1.35814871 pu, *i.e.* a rate of 2.97% < 3%, unlike nodes 3, 8 and 37 which respectively cause losses of 6.35%, 7.57% and 5.61%.

In sum, we note that in one or the other case, the joule losses in the entire Congolese power grid are within the norm.

Conflicts of Interest

The authors declare no conflicts of interest regarding the publication of this paper.

References

[1] Prisme (2001) Contrôle des pertes non techniques d'électricité. Institut de l'énergie et de l'environnement de la Francophonie (IEPF). Fiche technique No. 8.

[2] StéphaneGerbex (2003) Metaheuristiques Appliquees Au Placement Optimal De Dispositifs Facts dans un Réseau Electrique. Thèse de doctorat No. 2742. EPFL.

[3] Acha, E., Fuerte-Esquivel, C.R., Ambriz-Perez, H. and Angeles-Camacho, C. (2005)

FACTS: Modelling and Simulation in Power Network. John Wiley & Sons Ltd., Hoboken. https://doi.org/10.1002/0470020164

[4] Cheukem, A. and Ngundam, J.M. (2009) Implementation of FACTS Devices in Electrical Power System for Available Transmission Capability Enhancement. *International Journal of Numerical Methods and Applications*, **1**, 71-86.

[5] Srinivas, M. and Patnaik, L.M. (1994) Genetic Algorithms: A Survey. *Computer*, **24**, 17-26. https://doi.org/10.1109/2.294849

[6] Gogom, M., Mimiesse, M., Nguimbi, G. and Lilonga-Boyenga, D. (2018) Improving Availability of Transit Capacity by the Hybrid Optimization Method. *Journal of Scientific and Engineering Research*, **5**, 276-288.

[7] Sabonnadière, J.-C. and Hadjsaïd, N. (2007) Lignes et réseaux électriques. Lavoisier.

[8] Pal Barret, J., Bornard, P. and Mayer, B. (1997) Simulation des réseaux électriques. Editions EYROLLES.

[9] PA Consulting Group (USAID) (2005) Première Etude du Schéma Directeur pour l'Afrique Centrale.

[10] Direction Générale de l'Energie (2006) Schéma Directeur de Développement Industriel: Secteur Electricité. Ministère de l'Energie et de l'Hydraulique.

[11] Conseil Mondial de l'Energie (CME) (2008) Rapport sur l'Atelier de Haut Niveau du CME sur le Financement des Projets Hydroélectriques INGA, Tenu à Londres, le 21-22 avril 2008.

[12] Benras Med Amine, Larouisouleymane. Utilisation d'un dispositif STATCOM pour l'amélioration du transit de puissance d'un réseau de transport d'énergie alternatif, Mémoire de Master, 2015, Université KasdiMerbahOurgla, Algerie.

[13] Salim, H., *et al.* (2009) The Use of FACTS Devices in Disturbed Power System Modelling, Interface, and Case Study. *International Journal of Computer and Electrical Engineering*, **1**, 56-60. https://doi.org/10.7763/IJCEE.2009.V1.9

[14] Hassan, H.A., Osman, Z.H. and El-Aziz Lasheen, A. (2014) Sizing of STATCOM to Enhance Voltage Stability of Power Systems for Normal and Contingency Cases. *Smart Grid and Renewable Energy*, **5**, 8-18. https://doi.org/10.4236/sgre.2014.51002

[15] Ilango, R. and Raja, S. (2016) Fault Location Method for STATCOM Connected Transmission Lines Using CCM. *Circuits and Systems*, **7**, 3131-3141. https://doi.org/10.4236/cs.2016.710266

Annex 1: Congolese electricity grid data

We present here in Figure A1 the electrical map of Congo and in Figure A2 the Congolese electrical network integrated into the PEAC.

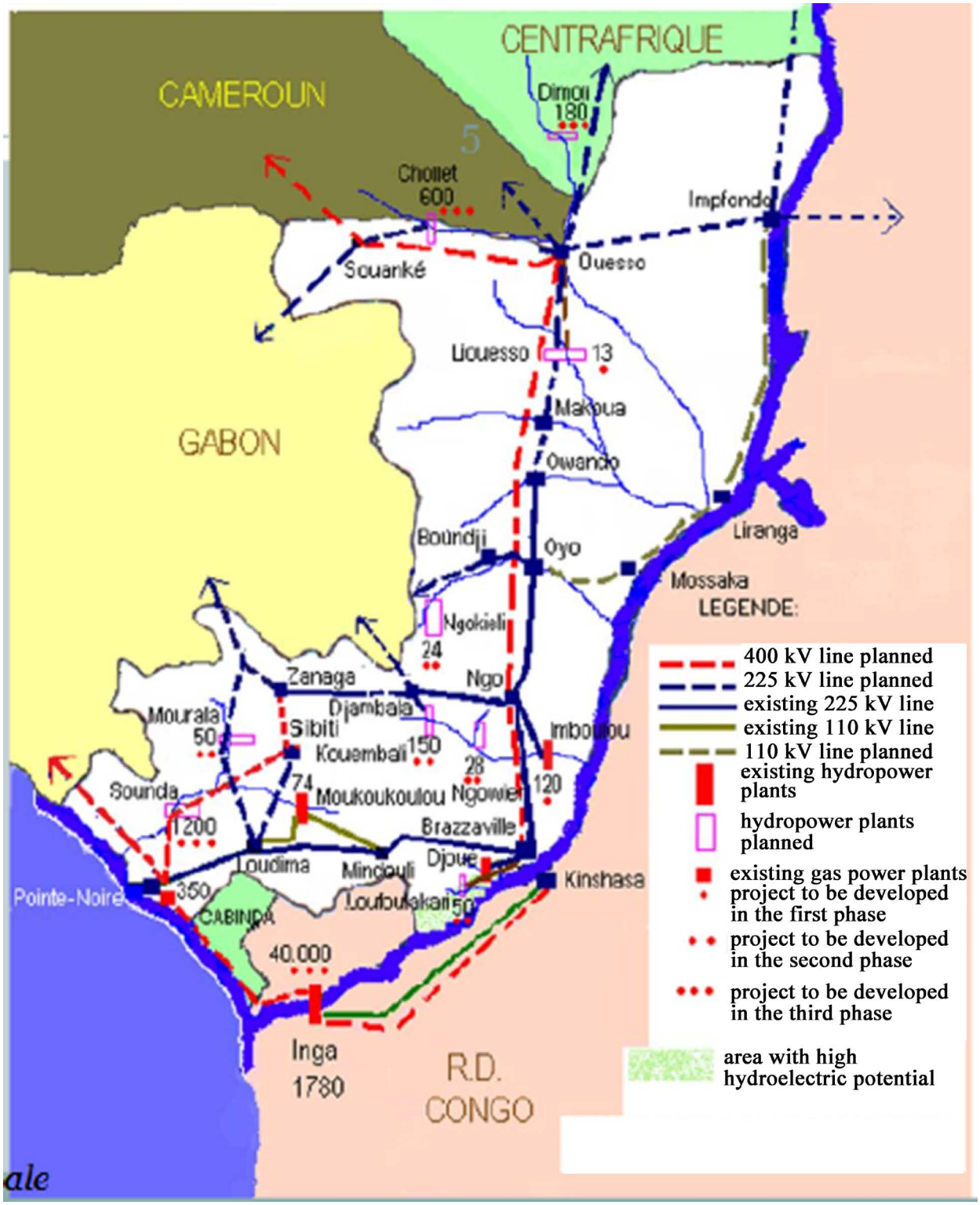

Figure A1. Congo Electric Map.

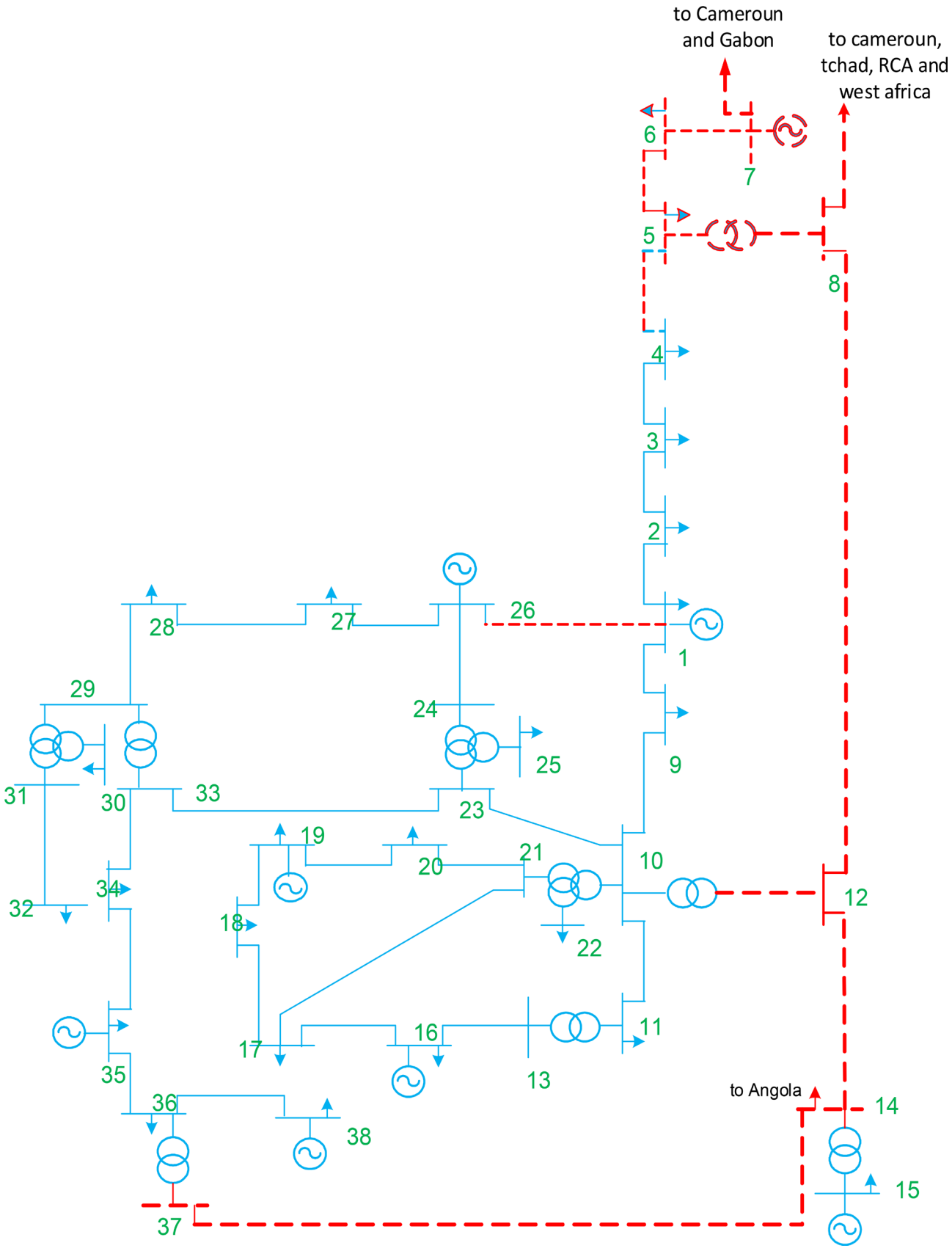

Figure A2. Diagram of the Congolese electricity network integrated into the PEAC.

Annex 2: Results

The results of simulations when the Congolese network absorbs electrical energy from the PEAC are presented in Table A1 and Table A2 below.

Table A1. Nodal electrical quantities.

Bus	V [p.u.]	phase [rad]	P gen [p.u.]	Q gen [p.u.]	P load [p.u.]	Q load [p.u.]
Bus01	1.05	0	0.47086117	2.31946878	0.4	0.248
Bus02	1.01829804	0.00693108	−4.1633E−15	−1.8513E−14	0.2	0.124
Bus03	1.00803123	0.01264462	1.6653E−16	4.563E−14	0.45	0.279
Bus04	1.00005618	0.02425556	3.9968E−15	2.8089E−14	1	0.62
Bus05	1	0.06615412	2.7833E−13	3.24823173	1	0.62
Bus06	0.95613086	0.1372357	1.5081E−12	4.1518E−12	3	1.58
Bus07	1.02	0.4947754	6	1.60804912	0	0
Bus08	1.00802162	0.18706557	6.1617E−15	5.4401E−15	0.5	0.31
Bus09	1.02	0.33122074	1.25	0.49294174	0	0
Bus09 (twt)	1.00182195	0.28518385	0	0	0	0
Bus10	1.01627756	0.32406793	3.6082E−15	−3.9635E−14	0.5	0.31
Bus11	1.01782609	0.3209317	−4.6647E−17	−7.2319E−15	0	0
Bus12	1.02	0.31722659	0.15	0.15645277	0.1	0.062
Bus13	0.99617294	0.25895503	−5.6621E−15	−1.0547E−14	0.5	0.31
Bus14	0.99956766	0.25942345	−4.7184E−15	5.3083E−14	0.15	0.093
Bus15	1	0.25958923	0.3	0.62695914	0.1	0.062
Bus16	0.99273044	0.26483313	−2.2204E−16	−1.5613E−15	0.1	0.062
Bus17	0.99754489	0.29783882	−1.119E−15	7.1241E−15	0	0
Bus18	0.9900241	0.26489371	3.3307E−16	−5.4956E−15	0.5	0.31
Bus19	1.01299911	0.33645666	−2.827E−14	−1.2622E−13	0	0
Bus20	1.01628828	0.34904393	−1.1959E−15	−2.591E−17	0	0
Bus20 (twt)	1.02085201	0.3271116	6.622E−17	−7.2536E−15	0	0
Bus21	1.01796677	0.32217383	−1.6653E−16	−1.4572E−15	0.1275	0.079
Bus22	1.02	0.40496601	0.72	−0.06375363	0	0
Bus23	0.98967952	0.34808349	1.027E−14	6.4906E−14	0.136	0.0843
Bus24	0.98952124	0.3463491	−6.6336E−15	−2.6625E−14	0.1	0.062
Bus25	0.9972036	0.33028481	−1.6781E−15	3.5477E−15	0	0
Bus25 (twt)	0.9868543	0.3140347	−4.3354E−17	7.0132E−15	0	0
Bus26	0.98918923	0.32019292	1.3508E−16	3.5134E−15	0	0
Bus27	0.9798509	0.30715948	2.7756E−17	−3.1086E−15	0.15	0.093
Bus28	0.98366611	0.30839625	5.5511E−17	−6.7724E−15	0.136	0.0843

Continued

Bus29	1.01017433	0.33867149	1.7605E−14	1.0967E−13	0	0
Bus30	0.98067267	0.38720397	1.1102E−15	−1.5543E−14	2	1.24
Bus31	1.02	0.45565847	4.5	1.13242573	0.02	0.0124
Bus32	1.01484848	0.42271807	−6.4393E−15	−1.2101E−14	1	0.62
Bus33	1.02	0.41105123	0.5	1.58313381	1.5	0.93
	Total powers		**13.8908672**	**11.1039092**	**13.6695**	**8.195**

Table A2. Losses in the lines.

Departure bus	Arrival bus	Line	P Loss [p.u.]	Q Loss [p.u.]
Bus01	Bus02	1	0.00095869	0.02114213
Bus02	Bus03	2	0.00103854	0.00186922
Bus03	Bus04	3	0.00139101	0.00584403
Bus04	Bus05	4	0.00383957	0.07242787
Bus05	Bus06	5	0.01563187	0.30515945
Bus06	Bus07	6	0.10755845	2.14274322
Bus01	Bus08	7	0.00405612	0.00774338
Bus08	Bus09	8	0.00240722	0.00556323
Bus09	Bus09 (twt)	9	0.00353321	0.04247134
Bus09	Bus10	10	0.00121752	−0.00204284
Bus09 (twt)	Bus17	11	0.0001662	−0.00452598
Bus09 (twt)	Bus18	12	−0.00051024	0.01389488
Bus09	Bus19	13	0.00125379	0.00778558
Bus10	Bus11	14	0.00011887	0.00078011
Bus11	Bus12	15	4.7326E−05	−0.01748126
Bus12	Bus13	16	0.00657444	0.00298508
Bus13	Bus14	17	0.00016016	−0.00262852
Bus13	Bus17	18	0.00247259	−0.00334371
Bus14	Bus15	19	2.9241E−05	−0.00015254
Bus15	Bus16	20	0.00010931	−0.00314586
Bus16	Bus17	21	0.00181131	−0.00507288
Bus19	Bus20 (twt)	22	0.00014164	−0.003857
Bus19	Bus29	23	0.0008555	0.0021875
Bus20	Bus20 (twt)	24	0.00073596	0.00884665
Bus20 (twt)	Bus21	25	−3.1371E−05	0.00085429
Bus20	Bus22	26	0.00701129	0.01322077
Bus22	Bus23	27	0.00845331	0.00931435

Continued

Bus23	Bus24	28	0.00013734	−0.00360195
Bus24	Bus25	29	0.00130122	0.00135679
Bus25	Bus25 (twt)	30	0.00051951	0.00624479
Bus25 (twt)	Bus26	31	3.9582E−05	−0.00107789
Bus25 (twt)	Bus28	32	−3.8234E−05	0.00104119
Bus25	Bus29	33	0.00023725	0.00532036
Bus26	Bus27	34	0.00039518	−0.02831079
Bus29	Bus30	35	0.00558001	0.02304082
Bus30	Bus31	36	0.02995397	0.20371215
Bus31	Bus32	37	0.00973448	0.06471416
Bus32	Bus33	38	0.00246935	0.01388707
Total loss			**0.22136117**	**2.90890919**

The simulation results obtained when the Congolese network injects electrical energy into the PEAC are presented in Table A3 and Table A4.

Table A3. Nodal electrical quantities.

Bus	V [p.u.]	phase [rad]	P gen [p.u.]	Q gen [p.u.]	P load [p.u.]	Q load [p.u.]
Bus01	1.02	−0.08990637	1.2	1.65101303	0.4	0.248
Bus02	0.99957515	−0.08309874	−8.0491E−16	2.8061E−14	0.2	0.124
Bus03	0.99361502	−0.07778674	7.7716E−15	5.2847E−14	0.45	0.279
Bus04	0.99069464	−0.06650662	3.8858E−15	3.5749E−14	1	0.62
Bus05	1	−0.02468612	8.058E−13	3.15754924	1	0.62
Bus06	0.95613086	0.04639546	3.9551E−12	9.8415E−12	3	1.58
Bus07	1.02	0.40393516	6	1.8925663	0	0
Bus08	1.00573151	−0.10555159	3.8858E−15	3.7192E−14	0.5	0.31
Bus09	1	−0.11084273	3.6637E−14	14.5824018	0	0
Bus09 (twt)	0.98977845	−0.15844268	1.6154E−15	−3.8191E−15	0	0
Bus10	0.9726693	−0.11963459	2.1316E−14	1.35E−13	29	15.276
Bus11	1.01597592	0.02485171	−1.1324E−13	6.839E−13	3	1.86
Bus12	1.02	0.03599956	25	4.94096046	0	0
Bus13	1.00104374	−0.11947222	−8.9928E−15	−3.1364E−14	0.5	0.31
Bus14	1.00928577	−0.12391194	3.1134E−15	−3.8778E−16	0	0
Bus15	1.02	−0.12832385	0.15	0.59052781	0.1	0.062
Bus16	0.99537043	−0.19003968	−4.6629E−15	−4.2411E−14	0.5	0.31
Bus17	0.99949471	−0.18968446	1.2712E−13	4.9966E−13	0.15	0.093

Continued

Bus18	1	−0.18952998	0.3	0.77446752	0.1	0.062
Bus19	0.9874159	−0.18389226	1.3045E−15	1.5613E−15	0.1	0.062
Bus20	0.97993931	−0.14602937	−4.3055E−16	6.3324E−17	0	0
Bus21	0.97782827	−0.17923593	−9.992E−16	5.7176E−15	0.5	0.31
Bus22	1.02471166	−0.03527128	1.2118E−14	7.2428E−14	0	0
Bus23	1.02642769	−0.02088728	−7.5975E−16	−3.6315E−15	0	0
Bus23(twt)	1.0368546	−0.04717133	1.1742E−16	7.37E−15	0	0
Bus24	1.03401452	−0.05195744	1.1102E−16	−3.8719E−15	0.1275	0.079
Bus25	1.02	0.04993334	0.72	−0.25243277	0	0
Bus26	1.0123579	0.00208377	−5.1348E−15	−8.2295E−15	0.136	0.0843
Bus27	1.0131423	0.00076963	1.1366E−14	2.4099E−14	0.1	0.062
Bus28	1.0336813	−0.01102473	−2.0723E−15	−1.0995E−14	0	0
Bus28 (twt)	1.02386176	−0.02614475	5.8908E−16	1.8178E−14	0	0
Bus29	1.02601492	−0.02042688	1.1389E−15	−2.3267E−17	0	0
Bus30	1.01713112	−0.0325471	−9.1593E−16	−5.565E−15	0.15	0.093
Bus31	1.02079059	−0.03138174	−5.5511E−17	−4.3437E−15	0.136	0.0843
Bus32	1.05	0	8.65764871	3.64049023	0	0
Bus33	0.9903157	0.05143973	1.1102E−15	−1.1102E−15	2	1.24
Bus34	1.02	0.12063377	4.5	0.80264618	0.02	0.0124
Bus35	1.01484848	0.08769338	2.6645E−15	−4.5186E−14	1	0.62
Bus36	1.02	0.07602653	0.5	1.58313381	1.5	0.93
	Total powers		**47.0276487**	**33.3633236**	**45.6695**	**25.331**

Table A4. Losses in the lines.

Departure bus	Arrival bus	Line	P Loss	Q Loss
Bus01	Bus02	1	0.00071896	0.01562483
Bus02	Bus03	2	0.00079833	0.0003731
Bus03	Bus04	3	0.00127651	0.00515473
Bus04	Bus05	4	0.00408284	0.07744503
Bus05	Bus06	5	0.01496751	0.29216087
Bus06	Bus07	6	0.11033549	2.19810752
Bus01	Bus08	7	0.00435453	0.01023328
Bus08	Bus09	8	0.00123606	0.00139634
Bus09	Bus09 (twt)	9	0.0033221	0.03993357
Bus09	Bus10	10	0.07773839	0.51015818

Continued

Bus09	Bus13	11	0.00137665	−0.0010526
Bus09 (twt)	Bus20	12	0.0002295	−0.00624983
Bus09 (twt)	Bus21	13	−0.00052305	0.01424365
Bus09	Bus22	14	0.1047277	0.71300615
Bus10	Bus11	15	0.77102902	3.17126108
Bus11	Bus12	16	0.0453166	0.29739019
Bus13	Bus14	17	0.00083061	0.0054509
Bus14	Bus15	18	0.00033624	−0.01154928
Bus15	Bus16	19	0.00731984	0.00448387
Bus16	Bus17	20	0.00023371	−0.00200302
Bus16	Bus20	21	0.00349657	−0.00043103
Bus17	Bus18	22	3.8077E−05	−7.7779E−05
Bus18	Bus19	23	0.00025879	−0.00186011
Bus19	Bus20	24	0.00237188	−0.00335134
Bus22	Bus32	25	0.13016904	0.36531299
Bus22	Bus23 (twt)	26	0.00027764	−0.00756053
Bus23	Bus23 (twt)	27	0.00119472	0.01436122
Bus23 (twt)	Bus24	28	−3.0405E−05	0.00082798
Bus23	Bus25	29	0.0113961	0.02636283
Bus25	Bus26	30	0.00489291	0.0009106
Bus26	Bus27	31	0.00011033	−0.00384938
Bus27	Bus28	32	0.00235443	0.00319298
Bus28	Bus28 (twt)	33	0.00047903	0.00575817
Bus28 (twt)	Bus29	34	3.6328E−05	−0.00098929
Bus28 (twt)	Bus31	35	−3.5504E−05	0.00096684
Bus28	Bus32	36	0.00039515	0.00886129
Bus29	Bus30	37	0.00036439	−0.03090029
Bus32	Bus33	38	0.01099716	0.05402413
Bus33	Bus34	39	0.02747072	0.18659458
Bus34	Bus35	40	0.00973448	0.06471416
Bus35	Bus36	41	0.00246935	0.01388707
	Total loss		**1.35814871**	**8.03232364**